

The Design of Tuned Front-End GaAs MMIC Optical Receivers

Stephen D. Greaves and Rodney T. Unwin

Abstract— Recently, much interest has been shown in the design of very low noise tuned front-end optical receivers for use in lightwave systems. This paper looks at the accurate design of such receivers. Simplified design expressions are presented for a number of tuning configurations with theoretical and measured results being presented. The designs were realized as GaAs monolithic microwave/millimeter-wave integrated circuits (MMIC's).

I. INTRODUCTION

THE use of front-end tuning in optical receivers can provide a significant improvement in the noise performance of certain optical communication links. Schemes such as subcarrier multiplexing (SCM) particularly benefit as the information to be transmitted is frequency translated before optical modulation. With such a modulation scheme the optical receiver only has to operate over a restricted bandwidth and as such allows tuned front-end techniques to be employed. A tuned front-end receiver not only provides the required passband response, but minimizes the noise contribution of the receiver. It is the design of such receivers that this paper considers.

The design of tuned front-end optical receivers using GaAs metal semiconductor field-effect transistors (MESFET's) has been investigated by several researchers. Simple series and parallel tuned designs have been considered by Gimlett [1]. More complicated structures were investigated by Alameh and Minasian [2] and Jacobsen [3]. All of these analyses predict a significant improvement in the noise performance by using tuning techniques, but all use simplified noise models of the device under consideration, typically the Ogawa Γ factor [4], and/or use ideal models of the tuning elements.

This paper first considers the noise model used in the analysis and concludes that the concept of a frequency independent noise parameter, such as the Γ used by Ogawa, is invalid when inductive front-end tuning is considered. It is shown that to design tuned front-end amplifiers correctly accurate values for the devices intrinsic noise parameters P , R , and C , are required. The work then investigates the four most common forms of front-end tuning, namely: series, parallel, pi and tee-tuning and provides simplified closed form analytic expressions for the tuning elements required. The degradation in expected noise performance due to the tuning networks thermal noise contribution is considered and it is concluded

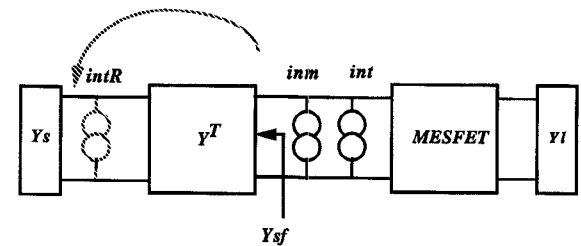


Fig. 1. Simplified model of a tuned front-end optical receiver.

that this can be the major source of noise in such a receiver. Two GaAs monolithic microwave/millimeter-wave integrated circuit (MMIC) designs are then presented and the measured results compared with the theoretical expectations.

A. Noise Modeling

The schematic of a tuned front-end optical receiver is shown in Fig. 1, where Y_s is the source admittance, typically this will be that of the PIN/APD and is almost totally capacitive. Y_l is the load admittance seen by the active device, which in this paper is a $0.5 \mu\text{m}$ gate-length GaAs MESFET. Y_{sf} is the admittance the tuning network presents to the device and Y^T is the admittance matrix that represents the tuning network. The total referred noise current generator $\overline{i_{ntR}^2}$ is described by

$$\overline{i_{ntR}^2} = \left| \frac{Y_{11}^T + Y_s}{-Y_{21}^T} \right|^2 (\overline{i_{nt}^2} + \overline{i_{nm}^2}) \quad (1)$$

where the super-scripted Y -parameters belong to the tuning network. $\overline{i_{nt}^2}$ represents the noise contribution of the active device and $\overline{i_{nm}^2}$ represents the noise contribution of the tuning network.

The purpose of the tuning network is to reduce $\overline{i_{ntR}^2}$ over the desired frequency range. In the analysis that follows the thermal contribution of the tuning network is initially neglected and all the noise is assumed to be that associated with the active device. This enables simplified tuning expressions to be produced for the tuning element values. The effect of the nonideal tuning network upon receiver noise performance will then be considered.

B. Active Device Noise Contribution

For the purpose of this analysis the model of the MESFET used is given in Fig. 2. This is the same model used by Ogawa in his analysis and initially appears to be a gross simplification. However, for the devices and bias conditions used in this paper it will be shown to be valid at frequencies up to 12 GHz.

Manuscript received June 29, 1995; revised December 18, 1995.

The authors are with The Communications Research Group, The University of Huddersfield, Huddersfield, West Yorkshire, UK.

Publisher Item Identifier S 0018-9480(96)02330-7.

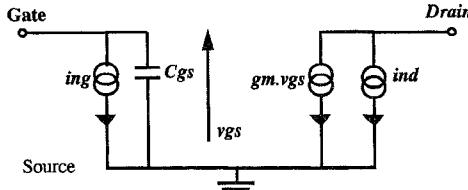


Fig. 2. Simplified MESFET noise model.

Based upon the model given in Fig. 2 the noise current spectral density that appears at the input to the device is given by

$$\overline{i_{nt}^2} = 4kTB \left(\frac{(\omega C_{gs})^2}{g_m} (P \cdot (K_{st})^2 + R - 2(\sqrt{PR} \cdot C \cdot K_{st})) + \frac{P \cdot (Re(Y_{sf}))^2}{g_m} \right) \quad (2)$$

where

$$K_{st} = 1 + \frac{Im(Y_{sf})}{\omega C_{gs}} \quad (3)$$

and

$$Y_{sf} = Y_{22}^T - \frac{Y_{21}^T \cdot Y_{12}^T}{Y_{11}^T + Y_s}. \quad (4)$$

In (2) k is Boltzmann's constant, T is absolute temperature in $^{\circ}$ Kelvin and B is the bandwidth. P , R , and C are the device intrinsic noise parameters [5]. P is the channel noise coefficient, R is the gate-induced noise coefficient while C is the correlation coefficient. The use of the intrinsic noise parameters P , R , and C is favored over the conventional extrinsic noise parameters, N_{fo} , R_n , and Γ_{opt} , as they have been shown to be sensibly frequency independent at frequencies below 30 GHz [6]. Equation (2) can be identified with Ogawa's expression but differs in two important ways. First, as Y_{sf} is totally capacitive in Ogawa's analysis, the term K_{st} is frequency independent, this yields the concept of the constant Γ factor. If Y_{sf} is inductive, which it is for the tuning networks considered here, this will no longer be true, thus violating the concept of the frequency independent Γ factor. Second, there is a significant term associated with the real part of the tuning network which can be dominant under certain resonance conditions. Of course, in (2) if Y_{sf} is totally capacitive, the expression reduces to Ogawa's original expression.

Before moving on the use of the simplified model proposed in Fig. 2 requires justification. Fig. 3 shows the expected noise performance of an F20 GaAs MESFET biassed for low-noise operation at $I_{DSS}/5$. The input termination is provided by a 0.5 pF capacitor, simulating the capacitance of a typical PIN diode. One set of results was generated using the full small signal model, such as that given in [7], while the second were generated using (2). Values for the intrinsic noise parameters, P , R , and C were extracted from noise measurements made upon the device of interest at the correct bias condition using the technique described in [7]. The results presented in Fig. 3 confirm that the simplified expression (2) adequately describes the noise performance of the active device up to 12 GHz.

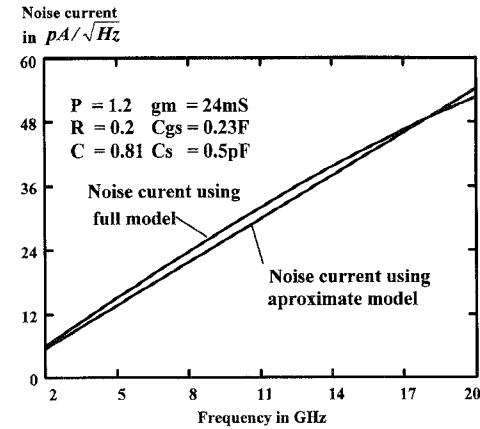


Fig. 3. Showing the noise performance of an F20 $0.5 \mu\text{m}$ gate-length GaAs MESFET when modeled with the full model and the simplified model.

C. Noise Reduction

Referring to Fig. 1, the noise contribution of the MESFET will be minimized if

$$-Im(Y_{sf}) = \omega C_{gs} \left(1 - \sqrt{\frac{R}{P}} \cdot C \right) \quad (5)$$

$$Re(Y_{sf}) = 0. \quad (6)$$

Under these conditions (2) reduces to

$$\overline{i_{nt}^2}_{\min} = 4kTB \left(\frac{(\omega C_{gs})^2}{g_m} R (1 - C^2) \right) \quad (7)$$

which represents the absolute minimum noise that can be achieved. This expression shows the importance of having a high correlation coefficient (C). This level of noise, however, appears at the input to the device and it is clear from Fig. 1 that this noise source must be referred to the input of the tuning network. This leads to the second tuning condition, namely that the term

$$Re f = \left| \frac{Y_{11}^T + Y_s}{-Y_{21}^T} \right|^2 \quad (8)$$

must be minimized. For minimum noise the tuning network must ensure that the two tuning conditions described by (5) and (8) must exist over the frequency range of interest.

II. ANALYTIC TUNING EXPRESSIONS

In other work, [2], [3], when the design of tuning networks is considered, it is usually from the viewpoint of computer optimization. If this approach is taken, then any understanding of the relationship that exists between the intrinsic noise performance of the device under consideration and the tuning network is lost. In this section, simplified closed-form expressions are given that enable the tuning element values of the four basic tuning configurations to be calculated directly. These configurations are parallel, series, equivalent pi, and equivalent tee tuning. The expressions derived also show how the tuning network element values are strongly dependent upon the active device's intrinsic noise parameters, P , R , and C .

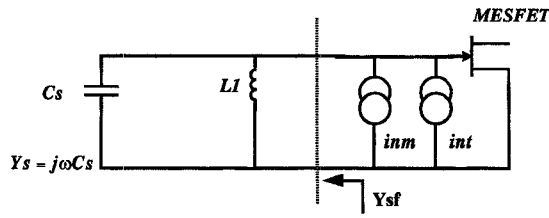


Fig. 4. Simple parallel tuned receiver.

A. Parallel Tuning

A simple parallel tuning network is shown in Fig. 4. Initially, to enable analytic tuning expressions to be derived, the tuning inductor is assumed to be ideal. In Fig. 4 the first tuning condition (5) is met if

$$L_{\text{opt}} = \frac{1}{\omega^2 (C_s + C_{gs} (1 - \sqrt{\frac{R}{P}} C))}. \quad (9)$$

Substituting (9) into (2) gives the minimum noise current

$$\overline{\text{int}R_{\text{min}}^2} = 4kTB \left(\frac{(\omega C_{gs})^2}{g_m} R (1 - C^2) \right). \quad (10)$$

It will be recalled that this represents the absolute minimum that can be achieved.

Clearly from Fig. 4 the referral term (8) has the value of unity and need not be considered.

B. Series Tuning

A simple series tuning network is shown in Fig. 5. Neglecting the real part of the tuning inductor, the referral term is given by

$$\left| \frac{Y_{11}^T + Y_s}{-Y_{21}^T} \right|^2 = (1 - \omega^2 C_s L)^2. \quad (11)$$

Using (5) and (11) the optimum value of tuning inductor is derived as

$$L_{\text{opt}} = \frac{1}{\omega^2 C_s} + \frac{P - \sqrt{P R C}}{\omega^2 C_{gs} (P + R - 2\sqrt{P R C})}. \quad (12)$$

The minimized value of total referred noise due to the device alone is then given by

$$\overline{\text{int}R_{\text{min}}^2} = 4kTB \left(\frac{(\omega C_{gs})^2}{g_m} R (1 - C^2) \right) \left(\frac{C_s}{C_{gs}} \right)^2 \cdot \frac{P}{P + R - 2\sqrt{P R C}}. \quad (13)$$

Comparing this expression with that derived for the parallel tuning case shows that using series tuning will incur a noise penalty of

$$\text{Penalty(dB)} = 10 \cdot \log \left(\left(\frac{C_s}{C_{gs}} \right)^2 \frac{P}{P + R - 2\sqrt{P R C}} \right) \quad (14)$$

with respect to the parallel tuning case. For a typical $0.5 \mu\text{m}$ gate-length GaAs MESFET biased for low-noise operation and having its input terminated with a PIN diode with capacitance $C_s = 0.8 \text{ pF}$, the penalty is around 12 dB.

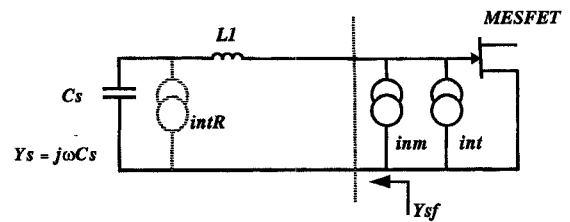


Fig. 5. Simple series tuned receiver.

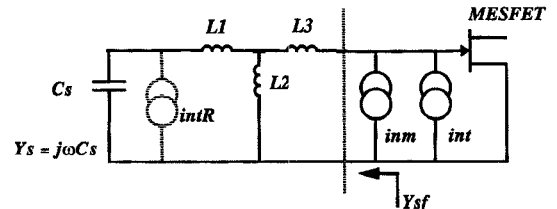


Fig. 6. Equivalent tee-tuned receiver.

C. Equivalent Tee-Tuning

When broader noise tuning bandwidths are required, multi-element tuning networks that provide a noise match across the desired frequency band are required. For tuning bandwidths of around an octave transformer tuning is a popular method used. The two equivalent circuit representations of a transformer, namely pi and tee are used when analyzing and designing transformer tuned front-ends. Initially, the equivalent tee-tuning network will be considered, such a network is shown in Fig. 6. Again, in order to develop analytic expressions for L1, L2, and L3 that will minimize the noise over the band of interest, it is initially assumed that the tee tuning network is ideal.

Considering the referral term first, with ideal components this reduces to

$$\left| \frac{Y_{11}^T + Y_s}{-Y_{21}^T} \right|^2 = \left(1 - \omega^2 C_s \left(L_1 + \frac{L_2 L_3}{L_1 + L_3} \right) \right)^2 \cdot \left(\frac{L_3}{L_2} + 1 \right)^2. \quad (15)$$

This clearly has a zero value when

$$L_1 + \frac{L_2 L_3}{L_1 + L_3} = \frac{1}{\omega^2 C_s}. \quad (16)$$

This is the first tuning constraint. As the network is initially considered to be ideal the referral term has the value of zero at this point. However, when dealing with nonideal inductors that have a finite Q the value of the referral term at the resonance point determined by (16) rises to

$$\left| \frac{Y_{11}^T + Y_s}{-Y_{21}^T} \right|^2 = \frac{1}{1 + Q^2} \left(\frac{L_3}{L_2} + 1 \right)^2 \quad (17)$$

where the value of Q can be approximated by the lowest Q in the network, clearly a high Q is desirable.

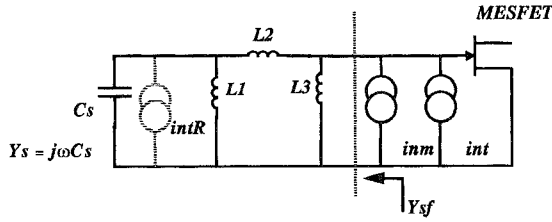


Fig. 7. Equivalent pi-tuned receiver.

Considering now the device noise term, this will be minimized if

$$-Im(Y_{sf}) = \frac{1 - \omega^2 C_s (L1 + L2)}{\omega (L3(1 - \omega^2 C_s (L1 + L2)) + L2(1 - \omega^2 C_s L1))}. \quad (18)$$

The two expressions (16) and (18) allow three equations to be developed in the three unknown inductor values. To do this the referral term (16) is chosen to have a resonance at the centerband frequency, while (18) is used to minimize the noise at the upper and lower bandedge frequencies. Solving these expressions for the three unknown inductor values gives

$$L1 = \frac{\omega u^2 + \omega l^2 - \omega c^2}{(\omega u \cdot \omega l)^2 C_s} - L2 \quad (19)$$

$$L2 = \frac{\sqrt{(\omega u^2 - \omega c^2)(\omega c^2 - \omega l^2)}}{(\omega u \cdot \omega l)^2 \sqrt{C_s \cdot C_{gs} \left(1 - \sqrt{\frac{R}{P}} C\right)}} \quad (20)$$

$$L3 = \frac{L2(1 - \omega l^2 C_s L1)}{\omega c^2 C_s (L1 + L2) - 1} \quad (21)$$

where ωl , ωc , and ωu are the lower, center, and upper bandedge frequencies, respectively.

D. Equivalent Pi-Tuning

A simplified equivalent pi-tuned front-end receiver is shown in Fig. 7. Again in order to develop analytic expressions for the prime inductor values $L1$, $L2$, and $L3$ the resistive part of each tuning inductor is ignored. Considering the referral term first

$$\left| \frac{Y_{11}^T + Y_s}{-Y_{21}^T} \right|^2 = \left(1 - \omega^2 C_s \frac{L1 \cdot L2}{L1 + L2} \right)^2 \cdot \left(\frac{L2}{L1} + 1 \right)^2. \quad (22)$$

This term clearly has a value of zero when

$$\frac{L1 \cdot L2}{L1 + L2} = \frac{1}{\omega^2 C_s}. \quad (23)$$

This is the first tuning condition. When dealing with a network using inductors having a finite Q the value of the referral term at resonance is no longer zero but rises to

$$\left| \frac{Y_{11}^T + Y_s}{-Y_{21}^T} \right|^2 = \left(\frac{L2}{L1} + 1 \right)^2 \frac{1}{Q_2} \quad (24)$$

where the value of Q can be approximated by the lowest Q in the tuning network and as in the tee-tuning network as higher Q as possible is desirable.

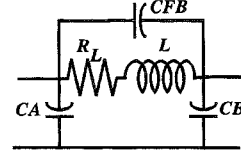


Fig. 8. F20 foundry spiral inductor model.

Considering the device noise term, again assuming ideal tuning components

$$-Im(Y_{sf}) = \left(\frac{1 - \omega^2 C_s L1}{L1 + L2(1 - \omega^2 C_s L1)} + \frac{1}{L3} \right) \frac{1}{\omega} \quad (25)$$

From which the minimum noise condition can be used to give the second noise tuning expression

$$\left(\frac{1 - \omega^2 C_s L1}{L1 + L2(1 - \omega^2 C_s L1)} + \frac{1}{L3} \right) = \omega^2 C_{gs} \left(1 - \sqrt{\frac{R}{P}} C \right). \quad (26)$$

As in the tee-tuning example the two expressions (24) and (26) allow three expressions to be developed in the three unknown inductors. Again the referral (24) term is chosen to resonate at the centerband frequency, while (26) is used to minimize the noise at the upper and lower band edges. Solving the expressions developed for the individual inductor values gives

$$L1 = \frac{\sqrt{\frac{C_{gs}}{C_s} \left(1 - \sqrt{\frac{R}{P}} C \right) \left(1 - \left(\frac{\omega l}{\omega c} \right)^2 \right) \left(1 - \left(\frac{\omega u}{\omega c} \right)^2 \right)} + 1}{\omega c^2 \left(C_s - C_{gs} \left(1 - \sqrt{\frac{R}{P}} C \right) \left(1 - \left(\frac{\omega l}{\omega c} \right)^2 \right) \left(1 - \left(\frac{\omega u}{\omega c} \right)^2 \right) \right)} \quad (27)$$

$$L2 = \frac{L1}{\omega c^2 C_s L1 - 1} \quad (28)$$

$$L3 = \frac{1}{\omega l^2 C_{gs} L1 - \sqrt{\frac{R}{P}} C - \frac{(1 - \omega l^2 C_s L1)}{L1 + L2 - 1 - \omega l^2 \cdot C_s L1}} \quad (29)$$

where ωl , ωc and ωu are again the lower, center, and upper band edge frequencies.

The expressions derived in this section for the four tuning networks are of interest as first, they give simplified closed-form expressions for the tuning element values, and second, they show that accurate values of the intrinsic noise parameters are required if the correct values of tuning element are to be obtained.

III. TUNING NETWORK NOISE CONTRIBUTION

In the expressions derived, the resistive part of the tuning inductor has been ignored. This is acceptable for the design of the tuning networks. It is not, however, acceptable to ignore the noise contribution of the tuning network, as this can be a dominant source of noise in these very low-noise designs. Equation (5) states that the tuning network must present an inductive susceptance to the active device over the frequency band of interest to achieve the minimum noise condition. The model of the F20 foundry spiral-inductor used in the GaAs MMIC designs considered here is shown in Fig. 8.

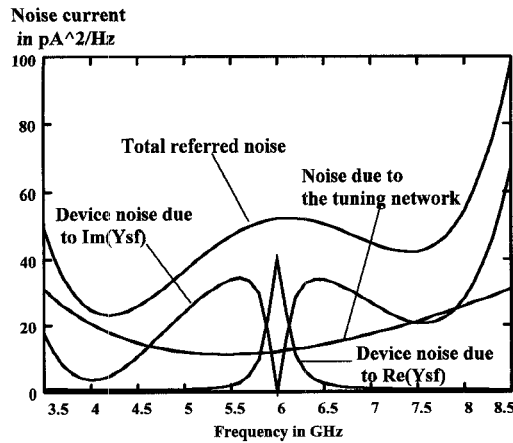


Fig. 9. Noise performance of a tee-tuned receiver, showing the effects of the nonideal tuning network.

To produce higher inductance values for a smaller spiral inductor size, the linewidth of the inductor is kept small. This leads to relatively high values (1 Ω –9 Ω) of series resistance. For the model shown in Fig. 8 this series resistance produces thermal noise that can be represented by a noise current generator with a spectral intensity given by

$$\overline{i^2} = 4kTB \frac{R_L}{R_L^2 + \omega L^2} = 4kTB Re(Y_L) \quad (30)$$

where Y_L is the admittance of the inductor.

The fact that the noise contribution of the inductor is related to the real part of the inductor admittance, is a statement of a more general relation that the noise contribution of any passive, lossy, linear network is proportional to the real part of the networks admittance/impedance. Thus the noise contribution of the tuning network shown in Fig. 1 can be described by

$$\overline{in^2} = 4kTB Re(Y_{sf}). \quad (31)$$

Fig. 9 shows the noise current spectral intensity of a 4 GHz–8 GHz tee-tuned amplifier with and without the thermal noise contribution of the tuning network. The uncharacteristic dip in the noise contribution of the active device due to the imaginary part of the source termination is clearly seen. This is not seen in other work where ideal tuning networks are assumed. At this point it is also clear that the device noise term associated with the real part of the tuning network is dominant noise term. The thermal noise contribution of the tuning network itself is also shown, and it can be seen that this term is a major source of noise in such a receiver and hence cannot be neglected. The total noise due to all sources is also shown and it can be seen that a significant degradation in the expected noise performance occurs when the real part of the tuning network is taken into account.

A. Practical MMIC Designs

In order to validate the design equations developed three tuned front-end receivers were produced and characterised, the results from two of which are reported here. The receivers were realized as GaAs MMIC's and fabricated by GEC/Marconi

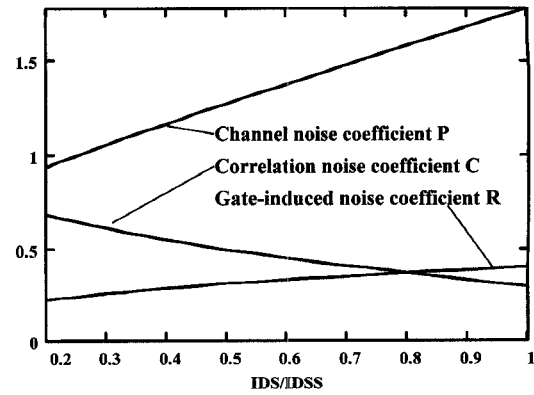


Fig. 10. Showing the variation of intrinsic noise parameter P , R , and C with bias for the device used.

using their F20 foundry process. In the designs that follow only the noise properties of the designs are considered, the broadband designs would require signal equalization but this is not considered here.

The first design is a parallel tuned front-end optical receiver having a noise minimum at 6 GHz, the second a tee-tuned front-end design having noise minimums at 2 GHz and at 4 GHz. The designs consist of the tuned front-end gain stage plus two further gain stages. The PIN diode capacitance was simulated on chip by a 0.5 pF capacitor. The following design procedure was adopted. First, the prime tuning inductor values were calculated using the equations developed in the previous section. The values for the intrinsic noise parameters used were extracted from measured extrinsic noise data using the technique outlined in [7] and were relevant to the device bias conditions used. The variation of the measured intrinsic noise parameters P , R , and C for the device under consideration with bias are presented in Fig. 10. Next, the circuit was laid out using the package CADENCE and the microwave simulator LIBRA used to optimize the overall amplifier noise response. Foundry simulator models were used to represent all the passive components, while the MESFET was modeled using a small signal model such as that given in [7]. The noise performance of the MESFET was modeled using both correlated and uncorrelated noise current generators. The uncorrelated noise sources depend upon values of the MESFET channel access resistances R_{gate} , R_{drain} , and R_{source} while the correlated noise sources depend upon the measured intrinsic noise parameters P , R , and C . A microphotograph showing the designs produced on one MMIC chip is presented in Fig. 11. The three designs run from the top of the chip to the bottom. The design on the far left is the 6 GHz design, in this design the input tuning can be seen in the bottom left, a second stage tuning inductor, shown mid-left on the chip, was also used in this design. The tee-tuned design occupies the central area of the chip. The tuning elements are clearly seen top center of the chip.

B. Measured Results: 2–4 GHz Design

Both the designs incorporate three gain stages. The first two stages are biassed for low-noise operation at $IDS = 10$ mA while the final stage is biassed at $IDSS = 50$

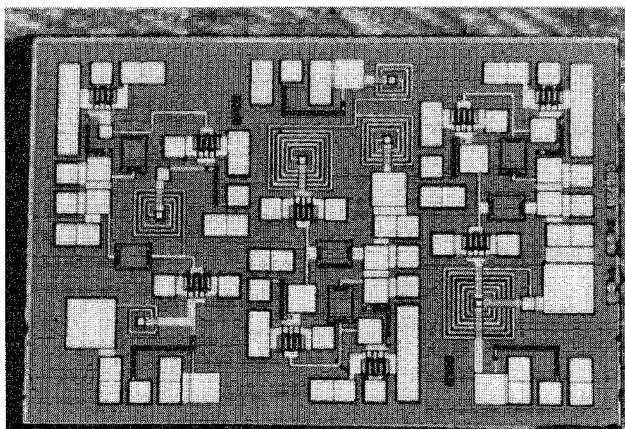


Fig. 11. Microphotograph of the MMIC chip produced. The chip contains three designs and has a total area of 6 mm^2 .

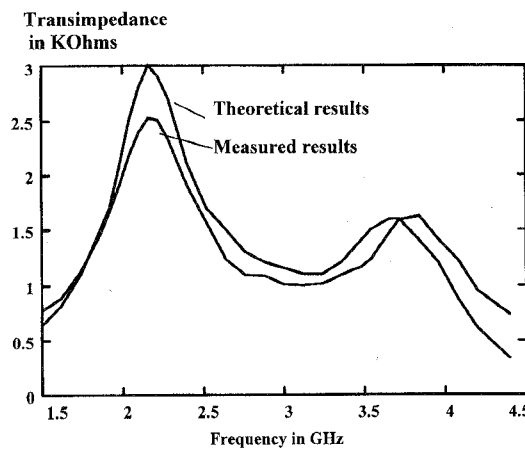


Fig. 12. Measured and theoretical receiver transimpedance, 2–4 GHz design.

mA. The prime inductor values calculated for this network are given in Table I along with the final Libra optimised inductor values. It can be seen that the optimised values are close to the prime inductor values, which validates the design expressions produced. Any discrepancy existing can be attributed to the $15\text{-}\mu\text{m}$ -wide transmission line interconnects and the fact that only multiples of one quarter integer turn inductors are available. The measured and theoretical values of receiver transimpedance and referred input noise current are shown in Figs. 12 and 13, respectively. These results were compensated for input stage loss and post amplification noise contribution, which in this case varied between -146 and -144 dBm/Hz in the band of interest. The measured input equivalent noise spectrum conforms well with theory, the measured and theoretical minimums occurring at the design frequencies. It can be seen that the measured results do deviate slightly mid band and it is felt that this is caused by the post amplification stage noise contribution introducing uncertainty into the measurement procedure.

C. Measured Results: 6 GHz Design

The 6 GHz design is close to the upper limit for parallel tuning using the F20 process. The value of tuning inductor

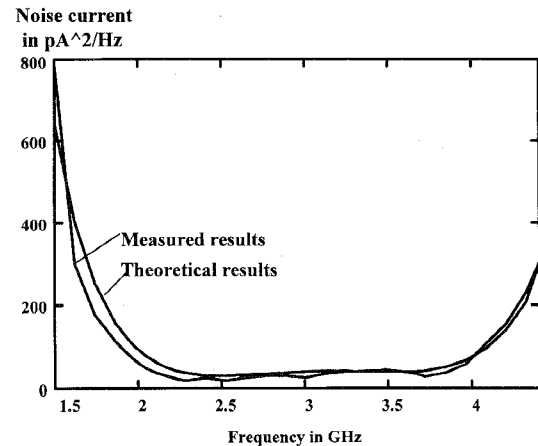


Fig. 13. Measured and theoretical receiver input noise current, 2 GHz–4 GHz design.

TABLE I
TEE-TUNED FRONT-END PARAMETERS

| $f_l(\text{GHz})$ | $f_c(\text{GHz})$ | $f_u(\text{GHz})$ | $c_s(\text{pF})$ | $c_{gs}(\text{pF})$ | $g_m(\text{mS})$ | P | R |
|-------------------|-------------------|--------------------|------------------|---------------------|------------------|--------------------|-----|
| 2 | 3 | 4 | 0.23 | 0.5 | 24 | 1.12 | 0.2 |
| C | $L1(\text{opt})$ | $L1(\text{prime})$ | $L2(\text{opt})$ | $L2(\text{prime})$ | $L3(\text{opt})$ | $L3(\text{prime})$ | --- |
| 0.81 | 0.831nH | 0.3nH | 7.86nH | 8.4nH | 12.28nH | 14.5nH | --- |

required with $C_s = 0.5 \text{ pF}$ is $L1 = 0.52 \text{ nH}$, which requires a 1.5 turn spiral inductor which is close to the one turn minimum. The initial value of inductor calculated using the expression given in (9) is 0.9 nH , which again justifies the simplified design approach. In this design, second stage matching was undertaken using a second tuning inductor. If this is not done, then the reflection coefficient that the tuned front-end transistor presents to the input of the second stage transistor causes the second stage noise to dominate.

The theoretical and measured values of receiver transimpedance are shown in Fig. 14, while the measured and theoretical values of receiver input equivalent noise current are shown in Fig. 15. A slight frequency shift of around 80 MHz is apparent in the transimpedance results which is well within the bounds allowed by the input network component tolerances. This shift is reflected in the noise current results, which, when the shift is taken into account, exhibit good correlation between measured and theoretical results with a minimum noise current of $70 \text{ pA}^2/\text{Hz}$ being achieved at 6 GHz.

IV. CONCLUSION

In this paper, the use of a simplified FET noise equivalent circuit in the design of tuned front-end optical receivers has been proposed. It has been shown that by using this approach, along with accurate values of the device's intrinsic noise parameters P , R , and C , results can be produced that are comparable with those obtained using a more complex equivalent circuit. This applies at frequencies up to at least 12 GHz. Using simplified tuning element models, analytic expressions for the tuning element values for four simple tuning configurations, namely parallel, series, pi and tee-

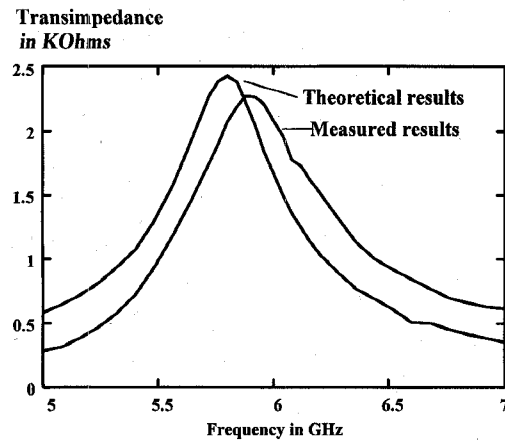


Fig. 14. Measured and theoretical receiver transimpedance, 6 GHz design.

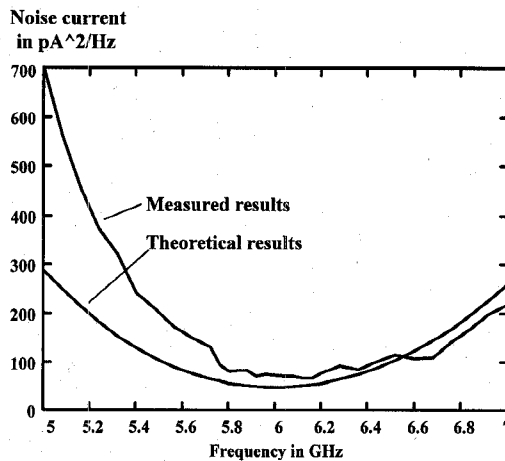


Fig. 15. Measured and theoretical receiver input noise current, 6 GHz design.

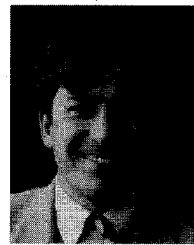
tuning, have been presented. These expressions rely heavily upon the intrinsic noise parameters through the noise scaling term $1 - \sqrt{\frac{R}{P}}C$. For narrow band tuning or spot frequency tuning it was shown that both series and parallel tuned front-ends are suitable although it was shown that series tuned front-ends suffer a noise degradation with respect to parallel tuning. For broadband tuning, it was shown that both equivalent tee and pi-tuning networks are suitable and again analytic expressions were produced for the tuning element values required. For all the networks produced it was found that a major source of noise in the receiver was that associated with the thermal contribution of the tuning network itself. Finally, practical measured results were presented that confirm the correctness of the design equations produced.

ACKNOWLEDGMENT

The authors wish to thank British Telecommunication Laboratories (BTL), the collaborating body.

REFERENCES

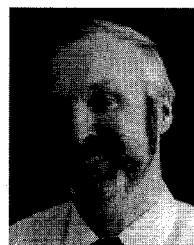
- [1] J. L. Gimlett, "Low-noise 8 GHz PIN/FET optical receiver," *IEE Electron. Lett.*, vol. 23, no. 6, pp. 281-283, Mar. 1987.
- [2] K. E. Alameh and R. A. Minasian, "Tuned optical receivers for microwave subcarrier multiplexed lightwave systems," *IEEE Trans. Microwave Theory Tech.*, vol. 38, no. 5, pp. 546-551, May 1990.
- [3] G. Jacobsen *et al.*, "Tuned front-end designs for heterodyne optical receivers," *J. Lightwave Technol.*, vol. 7, no. 1, pp. 105-114, Jan. 1989.
- [4] K. Ogawa, "Noise caused by GaAs MESFET's in optical receivers," *Bell Syst. Tech. J.*, pp. 923-928, 1981.
- [5] H. Statz *et al.*, "Noise characteristics of GaAs FET's," *IEEE Trans. Electron Devices*, vol. ED-21, no. 9, pp. 549-562, Sep. 1974.
- [6] B. Carnez, *et al.*, "Noise modeling in sub-micrometer gate FET's," *IEEE Trans. Electron Devices*, vol. ED-28, no. 7, pp. 784-789, July 1981.
- [7] S. D. Greaves and R. T. Unwin, "Accurate noise characterisation of short gate-length GaAs MESFET's and HEMT's for use in low noise optical receivers," *Microwave Optics Technol. Lett.*, vol. 6, no. 1, pp. 60-65, Jan. 1993.



Stephen D. Greaves is an Associate Member of the IEE.

Stephen D. Greaves was born March 23, 1962, in Wakefield, England. He received the B.Eng. (Hon.) degree in electrical and electronics engineering from Huddersfield Polytechnic in 1990, and the Ph.D. degree from the University of Huddersfield in 1994.

He is now a Senior Lecturer at the University of Huddersfield and coordinator for the Communications Research group. His research interests include noise modeling of active microwave devices, microwave measurements and optical receiver/system design.



Rodney T. Unwin received the M.Sc. degree in electronics from Southampton University in 1969 after being awarded an Electricity Supply Studentship. He received the Ph.D. degree from the University of Salford for work in the area of transistor noise modeling and measurement.

He was initially trained in the telecommunications industry in England. He later transferred to the electricity supply industry where he was employed as an Assistant Engineer, Telecommunications. Since 1972 he has been at the University of Huddersfield, where he is a Principal Lecturer and Leader of the Communications Research Group. He has authored and co-authored more than 65 papers, and his present research interests include low-noise electronics, optical fiber receivers, and systems and optical wireless systems.

Rodney T. Unwin is a Chartered Engineer and a Member of the IEE.